Available online at www.sciencedirect.com

ScienceDirect

Soils and Foundations 65 (2025) 101676

SOILS AND FOUNDATIONS

www.elsevier.com/locate/sandf

Seismic performance of an existing anchored quay wall in the Ravenna port (Italy) ☆

Pierluigi Alesiani [a], Paolo Ruggeri [b,*], Viviene M.E. Fruzzetti [b], Giuseppe Scarpelli [c]

[a] *Postdoctoral Researcher, Dipartimento di Scienze e Ingegneria della Materia, dell'Ambiente ed Urbanistica (SIMAU), Università Politecnica delle Marche, 60131, via Brecce Bianche 12, Ancona, Italy*

[b] *Associate Professor, Dipartimento di Scienze e Ingegneria della Materia, dell'Ambiente ed Urbanistica (SIMAU), Università Politecnica delle Marche, 60131, via Brecce Bianche 12, Ancona, Italy*

[c] *Full Professor, Dipartimento di Scienze e Ingegneria della Materia, dell'Ambiente ed Urbanistica (SIMAU), Università Politecnica delle Marche, 60131, via Brecce Bianche 12, Ancona, Italy*

Received 13 September 2024; received in revised form 25 June 2025; accepted 5 August 2025

Abstract

Evaluating the seismic performance of retaining walls is a significant engineering challenge due to non-linear soil-structure interaction, site response effects and ground motion properties. State of the art methods, based on non-linear dynamic analysis, are nowadays able to give reliable results when the numerical modeling is carried out with careful evaluation of seismic signals and appropriate choice of constitutive relationship for soils. However, a similar analysis is mostly restricted to relevant infrastructures. For large part of the practical situations, the simplified seismic analysis still represents the most used tool for design and verification. The new generation of Eurocode in Europe has introduced some innovations on the use of simplified seismic analyses making them more rationale and site-specific. In this paper, a case study involving the seismic evaluation of an existing anchored sheet-pile quay wall in the Ravenna port is presented. A well-known geotechnical setting and the data from an extensive field and laboratory investigation available for the area, allowed to perform both simplified and non-linear dynamic seismic analyses. The simplified seismic analysis according to the pseudo-static method outlined in the new draft of Eurocode 8 (FprEN1998:2024 TC250 – part 1 and 5), has been carried out and compared with the seismic performance of the quay wall evaluated through a 2D FEM non-linear dynamic analysis. Also, the seismic displacements of the quay wall from 2D FEM non-linear dynamic analysis were compared with recently proposed Newmark-type simplified methods. Relevant aspects of the presented case study are the very deep location of the bedrock, which required a separate model for site response analysis and 2D FEM non-linear dynamic analysis of the structures and the significant length of the wall embedment, due to poor geotechnical properties of the ground, which resulted in a pronounced spatial variation with depth of the ground motion.

Keywords: Site response; Pseudo-static method; Dynamic analysis; Case history; Anchored sheet pile quay wall; Performance-based design; Eurocode 8 draft

1. Introduction

Flexible retaining walls, such as anchored bulkheads and tieback walls, are very commonly adopted to sustain major excavations for infrastructures as well as to build vertical quay walls in port areas. The seismic response of waterfront structures is challenging due to non-linear soil-structure interaction, site response effects and ground

☆ This article is part of a special issue entitled: '8ICEGE-Osaka 2024' published in Soils and Foundations.

* Corresponding author.

E-mail addresses: p.alesiani@staff.univpm.it (P. Alesiani), p.ruggeri@staff.univpm.it (P. Ruggeri), v.m.e.fruzzetti@staff.univpm.it (V.M.E. Fruzzetti), g.scarpelli@staff.univpm.it (G. Scarpelli).

https://doi.org/10.1016/j.sandf.2025.101676

0038-0806/

motion properties (Kamon et al., 1996; Nozu et al., 2004; Sugano et al., 2014; Towhata et al., 1996; Iai, 2019). This is particularly true for anchored sheet-pile quay walls located on sites of poor geotechnical properties where the required embedment length of the structure is great and seismic site effect is relevant (Iai and Kameoka, 1993).

The use of advanced analysis methods, such as coupled non-linear dynamic analysis, allows to address these problems thanks to the availability of powerful computing resources and appropriate soil constitutive modeling. Therefore, it is now possible to obtain a complete evaluation of the seismic performance of geotechnical works, including both internal stresses and permanent displacements.

However, the general use of advanced analyses is not always technically and economically feasible and it remains limited to strategic projects. For these reasons, after an assessment of the stability of the construction site (i.e. hazards related to fault rupture, slope instability and liquefaction), designers typically rely on simplified seismic analyses for verifications in the majority of civil engineering projects. Simplified seismic analyses can in turn be divided in two main groups, namely pseudo-static methods and simplified dynamic (or displacement) methods.

The pseudo-static method of analysis, also known as static equivalent seismic analysis, is a traditional approach in which the real seismic action, variable in time and intensity, is reduced to an equivalent acceleration which is assumed constant in space and time. The method was first developed to obtain the seismic action for gravity wall by Mononobe and Okabe in the 1920s (Okabe, 1926; Mononobe and Matsuo, 1929) as a direct extension of Coulomb's earth pressure theory. According to this method, a pseudo-static inertial acceleration is applied on limit active (or passive) soil wedge. The earth pressure in seismic conditions (pseudo-static pressure) is therefore obtained through equilibrium equations for the forces acting on the soil wedge. The pseudo-static method has been applied to various design situations and it is also implemented in common commercial software based on the subgrade reaction method; this is achieved through the introduction of active and passive earth pressure coefficient evaluated by the Mononobe-Okabe formula. When a finite element model is considered, the method consists in the application of a constant horizontal acceleration to the entire domain of analysis, that corresponds to a deviation of gravity in the model.

Codes and recommendations usually give a guidance to define a pseudo-static acceleration for the design of retaining walls under seismic actions. The definition of such value is traditionally based on empirical rules that indicate the fraction of the peak ground acceleration to be considered in the seismic analysis. This means that the reliability of the seismic analysis mainly depends on the choice of an appropriate acceleration value, able to capture all the main factors influencing the seismic action. Recently, Codes (MLIT, 2020; CEN/TC 250/SC 8, 2024) are moving towards a more rational evaluation of the pseudo-static acceleration by considering the site response, the spatial variation with the depth of the horizontal ground motion within the ground mass under consideration (i.e. a non-uniform motion in the volume of interest) and the amplitude of accepted permanent displacements of the soil structure system (i.e. a ductile dissipation of the seismic energy). The new Eurocode 8 has been extensively updated on seismic design and the pseudo-static method has been revised to improve user awareness and reliability of results (Pecker, 2019).

Simplified dynamic methods (or displacement methods) refer back to Newmark's well known rigid block analysis (Newmark, 1965). This method, developed for the evaluation of the seismic behavior of earth dams, was first applied to gravity retaining walls (Richards and Elms, 1979; Nakajima et al., 2009) and then extended to sheet-pile walls (Towhata and Islam, 1987; Cecconi et al., 2015; Conti and Viggiani, 2023), for the translation mode. Essentially, following the displacement method, the critical acceleration (i.e. the value of the seismic acceleration related to the activation of a collapse mode of the geotechnical system) is evaluated and, by integrating twice the value of the seismic signal beyond this triggering threshold, the permanent displacement of the structure is estimated. The original method assumed a rigid perfectly-plastic behaviour of the soil, so the evaluation of the permanent displacements was approximate for all situations in which this hypothesis was not realistic. Focusing on embedded retaining walls, several research studies improved the method by including the deformability of the soil and the progressive mobilization of soil passive strength; these two components drive the accumulation of permanent displacements even before the attainment of the critical acceleration. Two families of methods, capable of addressing the limitations outlined, have been recently proposed for the computation of permanent displacements during earthquakes of embedded retaining walls: the non-linear SDOF model (Callisto, 2019) and the Generalized Newmark Method (Cattoni et al., 2019; Oliynyk et al., 2022; Caputo et al., 2023).

In this paper, the seismic performance of an existing anchored sheet-pile quay wall in the Ravenna port area is evaluated both using the simplified seismic analyses (i.e. both pseudo-static and displacement methods) and the non-linear dynamic analysis carried out through a 2D finite element model (see also Alesiani et al., 2024a; Alesiani et al., 2024b). The pseudo-static analysis is developed according to the procedure adopted by the new Eurocode 8. The Generalized Newmark Method with Hardening (GNMH) is applied for the simplified evaluation of the seismic displacements of the anchored retaining walls. The main objective is to explore the potential of the most recent simplified method in evaluating the seismic response of a retaining structure that, due to embedment length, soil condition, depth of bedrock, does not represent the typical situation for which these methods were developed and tested. The quay of interest is an anchored steel sheet-pile wall, with the main steel profiles extended up to 27.5 m below m.s.l., capable of operating with a seabed at 11.5 m b.m.s.l and a surcharge of 40 kPa, built on recent soils characterized by poor geotechnical properties.

2. Methods

2.1. Pseudo-static analysis: Equivalent acceleration according to Eurocode

According to the second generation of Eurocode 8 part 5 (CEN/TC 250/SC 8, 2024), the seismic action for pseudo-static analysis of geotechnical structures is defined by a conventional horizontal ground acceleration:

$$a_H = \frac{\beta_H}{\chi_H} PGA_e \tag{1}$$

where:

β_H is a coefficient reflecting the spatial variation with depth of the horizontal ground motion within the ground mass under consideration;
PGA_e is the design peak value of horizontal ground acceleration;
χ_H is a coefficient reflecting the amplitude of accepted residual displacements for the considered limit state.

The Eurocode also introduces a methodology in which the influence of site effects and spatial variation of the ground motion with depth within the volume of interest of the system are evaluated directly from the results of a site-specific ground response analysis. In this case, the term $\beta_H PGA_e = \bar{a}_{eq}$ can be calculated from the formula:

$$\bar{a}_{eq} = \frac{g}{\sigma_{v,H}} \frac{\sum_{i=1}^{n} [\max \tau_{i,H}(t)]}{n} \tag{2}$$

where:

$\bar{a}_{eq}$ is the average value of the equivalent acceleration;
$\max \tau_{i,H}(t)$ is the maximum value of the shear stress calculated with the ith accelerogram at a reference depth H;
$\sigma_{v,H}$ is the total vertical stress at a depth H;
n is the number of accelerograms used in the analysis.

The relevance of the reference depth H to be selected for the different types of retaining walls is evident. In the informative Annex A of the Eurocode, for embedded retaining wall, the reference depth H is indicated as the wall height when the active side is considered and the embedment length for the passive side.

2.2. Simplified dynamic methods (displacement methods)

A convenient procedure for the computation of earthquake-induced permanent displacements of retaining structures is to decouple the dynamic soil-structure interaction problem. The seismic input can be evaluated in free-field conditions performing an equivalent-linear or non-linear site response analysis. Then, an equation of motion based on a simplified model of the soil-structure system is solved to compute the seismic displacements of the wall. To this end, the sliding block model (Newmark, 1965) is commonly used.

Recent works have extended the classical formulation of Newmark's method to overcome known shortcomings when applied to the evaluation of permanent seismic displacements of anchored sheet-pile walls. In particular, the rigid-perfectly plastic block model allows accumulation of displacements only for values of acceleration greater than the critical acceleration that activates the plastic mechanism of the soil-structure system. The pre-failure displacements, due to the progressive mobilization of soil passive resistance from the initial static condition to the full activation of the plastic mechanism, are therefore neglected in the original formulation (Callisto, 2014).

Another issue concerns the acceleration time-history to be used as base acceleration for the sliding block. When the results of a site response analysis are available, the choice usually falls on the free-field acceleration at ground surface, although two dimensional effects and spatial variability of the seismic motion within the volume of soil influencing the wall could considerably alter the dynamic response of the system.

The pre-failure non-linear behaviour of the system can be simplified by a pseudo-static pushover response curve, also known as capacity curve, which defines the progressive mobilization of the system strength with displacement as the acceleration increases up to the critical value. A hardening law for the critical acceleration based on the capacity curve can then be implemented in the Newmark double integration procedure to include this contribution to the final permanent displacements, as shown by Oliynyk et al. (2022) and Caputo et al. (2023).

Finally, regarding the acceleration time-history $a_B(t)$ to be used in the computation, Callisto (2024) suggested to perform a one-dimensional site response analysis and obtain an equivalent accelerogram as proposed by Seed and Martin (1966) for earth dams:

$$a_B(t) = a_{eq}(t) = g\frac{\tau_H(t)}{\sigma_{v,H}} \tag{3}$$

where $\tau_H(t)$ is the shear stress time-history at the depth H of the soil column equal to the depth of the wall and $\sigma_{v,H}$ is the vertical total stress at the same depth. This allows to take into account in a simplified way the vertical variability of the horizontal ground acceleration along the wall height, similarly to that expressed by Eq. (2).

2.2.1. Capacity curve

The seismic capacity of a retaining wall can be evaluated through a pseudo-static numerical analysis by applying progressively increasing inertial forces, proportional to the horizontal seismic coefficient k_h, to a suitable non-linear model. The relationship between the seismic coefficient and the displacement of the wall can be conveniently represented in a non-dimensional form using the hyperbolic expression proposed by Callisto (2019):

$$k_h = \frac{sk_c}{s\alpha + s_F(1-\alpha)} \tag{4}$$

where s is the normalized displacement at the control point u_r/H, k_c is the critical seismic coefficient, s_F is the value of the normalized displacement when the failure mechanism is activated and $\alpha < 1$ is a best fitting parameter defining the asymptote of the hyperbolic function.

Callisto (2019) and Caputo et al. (2023) observed that the shape of the capacity curve mainly depends on the system deformability and proposed the typical parameters range for ideal layouts of different types of retaining walls.

2.2.2. Generalized Newmark method with hardening (GNMH)

The Generalized Newmark Method (GNM) by Cattoni et al. (2019) was developed to estimate the permanent displacement field of retaining structures subjected to seismic action, for generally complex plastic mechanisms. The method relies on the use of a pseudo-static numerical analysis to compute the critical acceleration a_c of the system and to identify the soil volume involved in the failure, for which the full displacement field is derived through a Newmark-like scalar dynamic equation of motion and proper assumptions.

Following the formulation of GNMH by Caputo et al. (2023) to account for the initial non-linear behaviour of the soil-wall system, the seismic permanent displacement at the top of the wall is defined as:

$$u_r = -\eta^{GN}{}_{\dot{u}_r>0}[a_B(t) - a_c]dt^2 \tag{5}$$

where the coefficient η^{GN} is an integral quantity, depending on the total mass and the resultant normalized momentum of the failing soil volume, which inherently accounts for the type of plastic mechanism. The normalized horizontal displacement field of the soil volume $\mathfrak{B}_f$ involved in the failure mechanism is defined as:

$$\lambda_x(\boldsymbol{x}) = \frac{\boldsymbol{u_r}(\boldsymbol{x})}{max\|\boldsymbol{u_r}(\boldsymbol{x})\|} \tag{6}$$

and includes all volume elements characterized by $\|\lambda_x(\boldsymbol{x})\| \geq TOL$ in which TOL is the assumed tolerance value. The total mass M and the resultant normalized momentum of the body $\mathfrak{B}_f$ in horizontal direction are:

$$M = \int_{\mathfrak{B}_f} \rho dV$$

$$Q_x = \int_{\mathfrak{B}_f} \rho \lambda_x(\boldsymbol{x}) dV \tag{7}$$

where ρ is the density of soil.

Then, the coefficient η^{GN} is given by:

$$\eta^{GN} = \lambda_x(\boldsymbol{x}_{TOP})\frac{M}{Q_x} \tag{8}$$

where $\boldsymbol{x}_{TOP}$ is the position of the top of the wall. It depends on the geometry and strength of the system, taking into account the continuous displacement field through $\lambda_x(\boldsymbol{x})$, providing an accurate description of the kinematic mechanism at failure. The full analytical derivation of the formula can be found in Caputo et al. (2023) and Cattoni et al. (2019).

The pre-failure deformability of the soil-wall system is introduced through a displacement-hardening law (Eq. (9)) for the critical acceleration a_c, that is no longer assumed constant but evolves according to the hyperbolic function of the capacity curve in Eq. (4). In this way, the mobilized critical acceleration $a_c^{(m)}$ is zero at the initial time steps of the acceleration time-history and progressively increases with the accumulation of horizontal displacements at the top of the wall – and so the system strength – over the earthquake duration:

$$a_c^{(m)} = \begin{cases} \frac{sa_c}{s\alpha + s_F(1-\alpha)} & for\ s < s_F \\ a_c & for\ s \geq s_F \end{cases} \tag{9}$$

3. Case study

The case study of interest is a quay wall located along the Candiano Channel of the Ravenna port, in Italy. Built in the early 2000s for the purpose of widening the port channel, the structure was driven backward with respect the old channel bank and designed to more demanding operational requirements: a seabed at 11.50 m below m.s.l. – with the apron at 1.5 m a.m.s.l. – and an operative surcharge of 40 kPa.

3.1. Ground model

The area of interest belongs to the coastal part of the Po Plain (northern Italy), so the seismic bedrock is very deep and not reached by typical surveys.

Differently, soil properties of the first 40–50 m are based on the results of several laboratory and in situ testing (including CPTs, DMTs, triaxial and oedometer tests, geophysical and resonant column tests). It turns out that the soils in the volume of interest are Holocenic deposits of marine origin laying on Pleistocene alluvial soils. As shown in Fig. 1, the Holocenic sequence can be grouped in 3 Units: from the ground surface we find a medium dense Silty Sand (S) layer, 14 m thick, followed by a very soft Clayey Silt (M) deposit up to a depth of 26 m. A 2 m thick layer of Sand (T-Sand) indicates the transition to the Pleistocene soils of alluvial plain (Alluvial Soil, AES7-1), constituted by a sequence of fine and coarse-grained layers of generally good mechanical properties.

a)

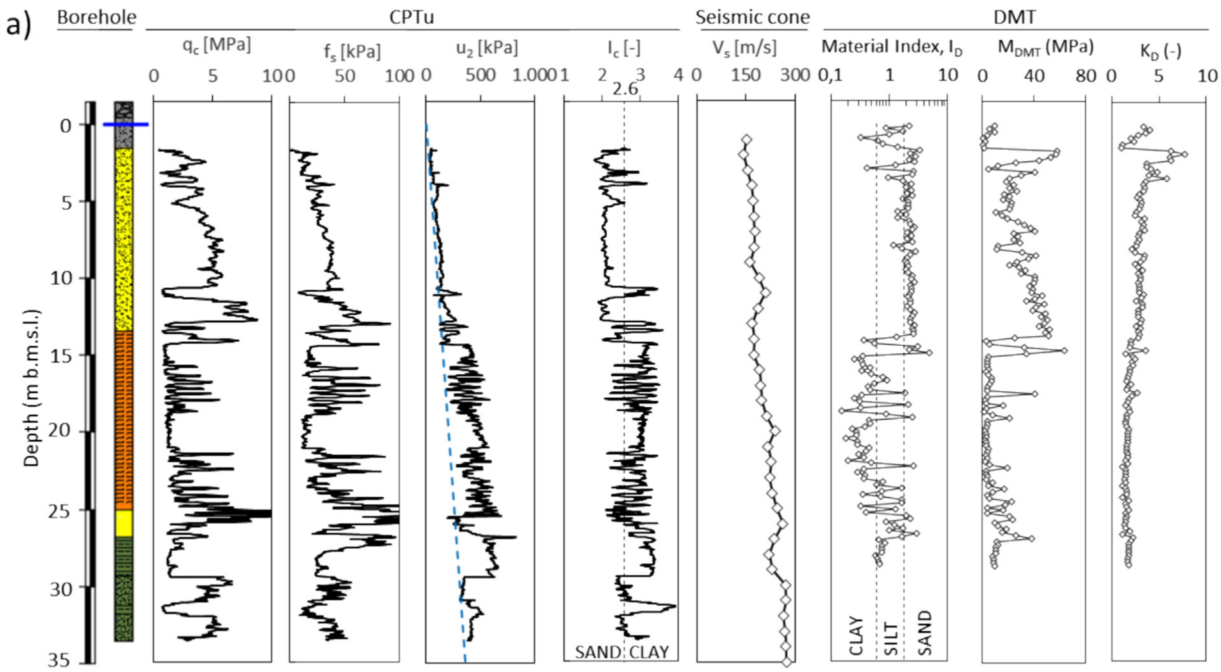

b)

Geotechnical Unit		Silty Sand (S)	Clayey Silt (M)	Tran. Sand (T)	Alluvial Soil (AES7-1)
Param.	Unit				
γ	kN/m^3	17.5 - 18.5	17.5 - 19.5	18.5 - 19.5	19.0 - 20.0
LL	%	-	30 - 50	-	32 - 57
PI	%	-	10 - 30	-	12 - 33
OCR	-	-	1	-	1 - 2
c'	*kPa*	0	0	0	0
φ'	°	32 - 38	28 -32	32 - 38	26 - 32
s_u	*kPa*	-	20 - 50	-	60 - 110
E_{50}	*MPa*	10 - 20	-	10 - 20	-
E_{oed}	*MPa*	-	2 - 6	-	8 - 20
G_0	*MPa*	25 - 70	35 - 80	70 - 100	80 - 120

c)

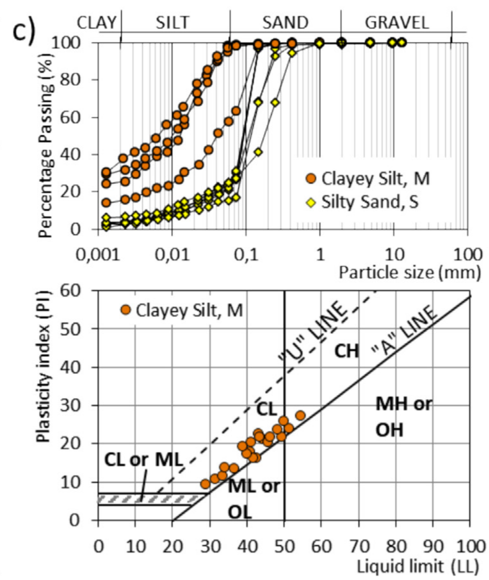

Fig. 1. Typical geotechnical properties of the soils in the first 35 m from ground surface: a) Representative borehole with identification of the main layers, data from CPTu, DMT results; shear waves velocity profile from Seismic cone; b) Geotechnical properties of the main Geotechnical Units; c) Particle size distribution curves of Silty Sand (S) and Clayey Silt (M) and Atterberg Limit of Clayey Silt on the Plasticity Chart.

In Fig. 1a, aligned to a typical borehole log carried out in the area, the main data obtained from a piezocone penetrometer testing, the main results from a flat dilatometer test and the shear wave velocity profile from a seismic cone are shown. The distinction between the different units is clearly recognizable by examining the test results: the Silty Sand (S) is characterized by a cone tip resistance ranging from 3 to 5 MPa and a permeability high enough to prevent the development of excess pore pressure during penetration; the transition to the Clayey Silt (M) is identified by a sudden drop in tip resistance and a clear development of excess pore pressure; the T-Sand is recognised by a new peak in tip resistance, associated with the disappearance of excess pore pressure; the Alluvial Soil, investigated for only few meters, is characterized by an alternating sequence of sand and clay layers. The Soil Behaviour Index derived from CPTu and DMT tests are consistent with the soil identification obtained from the borehole logs. In Fig. 1b, the general properties of the main geotechnical units, derived from various in-situ and laboratory tests, are summarised. Focusing on the Silty Sand and Clayey Silt layers, which are the most critical for the design of the works in the area, Fig. 1c presents the typical soil particle distributions; on the Plasticity Chart, the Clayey Silt samples align close to the "A-line", falling within the "Low Plasticity Clay" (CL) classification.

The soil stratigraphy below the investigated depth has been reconstructed based on the geological model of the area derived from previous studies. In particular, according to the data provided by the Emilia Romagna region and specific studies aimed at defining a seismic model for the port area of Ravenna, the seismic bedrock is assumed at a depth of 350 m. Also, the regional map provides some geological sections and a simplified stratigraphy for the main layers between about 50 and 350 m (ISPRA, 2009). Fig. 2 shows the assumed stratigraphical model of the area used for the following analysis, along with the geotechnical cross-section of the quay wall (see for further details Alesiani and Ruggeri, 2024; Senigagliesi et al., 2024).

3.2. Seismic stability of the construction site

It is well known that construction sites may be affected by fault rupture, slope instability, and permanent settlements caused by liquefaction or significant densification under seismic action. Past experience has demonstrated the high vulnerability of port infrastructures to earthquake damage (PIANC, 2001). This is due to several contributing factors, such as the relevant height of quay walls, the recent geological origin of the soil that characterizes many harbor areas – often located near river mouths – and the expansion of ports through reclamation land activities. These factors make port areas particularly prone to liquefaction under seismic shaking, a phenomenon able of causing severe damages to structure such as quay walls, caissons, breakwaters, piers (Sumer et al., 2007). For this reason, current guidelines provide clear recommendations for evaluating the liquefaction susceptibility of a site prior to construction, requiring soil improvement interventions to compact loose sandy sediments as well as remedial measures against liquefaction, such as drainage methods. Analysing in detail several case histories of severe seismic liquefaction occurred in port areas, some authors (Towhata, 2008; Kayen, 2024) pointed out the role of surface geology to differentiate the very high liquefaction potential of young artificial deposits or backfill of sand from natural deposits of sand that are at least hundreds of years old.

In the current case study, the natural deposit where the quay wall of interest is located shows a potential risk of liquefaction. Depending on the earthquake return period and the analysis method adopted, this risk is assessed as low to medium. No specific mitigation measures against liquefaction were implemented. The structure was built approximately 20 years ago, when liquefaction hazards were rarely considered in Italian geotechnical practice. Current geotechnical design standards routinely address liquefaction susceptibility, and mitigation techniques—such as stone columns or jet-grouting treatments—are sometimes employed, especially for strategic infrastructure. Furthermore, the liquefaction potential of the sandy soil deposit in the Ravenna port area remains a subject of debate due to its natural origin, the region's relatively low seismicity, and the soil's cyclic resistance.

In the following analysis, the Hardening Soil model with Small-Strain Stiffness (HSsmall) is employed in 2D finite element dynamic simulations. While this model is widely used in seismic geotechnical analyses, it does not allow for a realistic simulation of excess pore pressure generation and dissipation, potential soil liquefaction or cyclic strength degradation. As a result, the present study does not address these aspects, and the numerical results must be interpreted with this limitation in mind.

When liquefaction is expected to play a significant role, the use of more appropriate constitutive models becomes necessary, as discussed by Oliynyk et al. (2021).

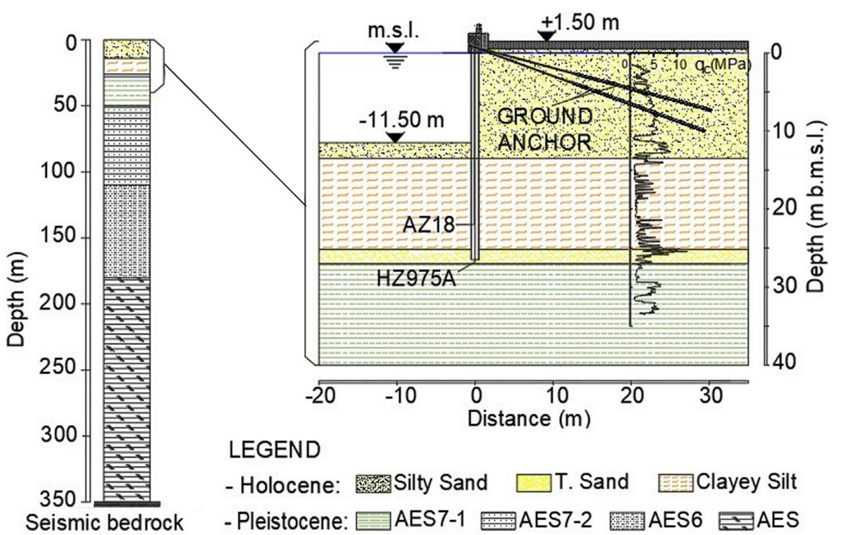

Fig. 2. Simplified stratigraphical model and the geotechnical cross-section of the sheet-pile quay wall.

3.3. Structure description

The quay is a combined steel sheet pile coded as HZ975A-12/AZ18, with an H-shaped king pile and Z-shaped intermediate profiles. The sheet pile is composed of steel profiles joined at the top by a 1.6 × 2.5 m (B × H) concrete beam hosting the heads of grouted anchors which provide the necessary constraint at the top of the retaining wall. Each anchor has a total length of 32 m (14 m free and 18 m fixed) with an alternating inclination from the horizontal of 15° and 20° and are reinforced with 5 strands of 0.6″ each. The safety factor (SF) against general failure of the quay wall, evaluated under static conditions using the phi/c reduction procedure, assuming drained behavior and characteristic parameters for all soils, without surcharge, is close to 2.5. The value of SF depends on the embedment depth of the wall, which was extended down to the Alluvial soil to avoid the stability problems experienced by shorter quay walls in the port area.

3.4. Seismic data

The Italian Building Code NTC2018 provides the 5 %-damped elastic design spectra for eight return periods, between 50 and 10,000 years, on ground type A (i.e. without soil amplification), for every location. In Fig. 3 the target spectrum for the site of Ravenna, on ground type A and return period of 475 years, is shown. The return period of the seismic action is based on a 10 % probability of exceedance over 50 years (which corresponds to the nominal lifespan of the structure) and represents the standard value typically adopted for verification procedures in Italy. In the same graph, the 5 %-damped elastic response spectra of 7 selected accelerograms, whose mean response spectrum matches that of the NTC2018, are also shown.

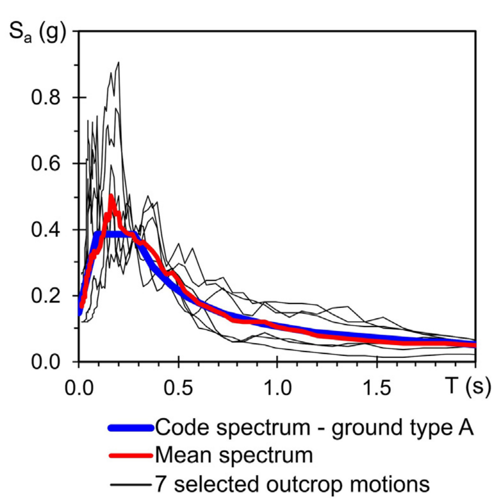

Fig. 3. Spectral matching verification of 7 scaled ground motions with target spectrum provided by Italian Building Code.

The set of 7 accelerograms was taken from the work of Rota et al. (2012) who carefully selected set of recorded seismic signals characterized by low scaling factor and by the exclusion of dominant earthquakes (i.e. records whose response spectra differ significantly from the target spectrum).

The main properties of the chosen accelerograms are listed in Table 1.

3.5. Numerical models

The numerical analyses of the geotechnical system of interest have been carried out including three models: i) the 1D equivalent-linear model on a column extended up to the seismic bedrock (i.e. 350 m); ii) the 1D non-linear model extended up to "engineering bedrock" (i.e. 58 m); iii) the 2D FEM model that has been adopted for non-linear dynamic analysis and pseudo-static FE analysis. The conceptual scheme is represented in Fig. 4. According to the "Technical standards and commentaries for port and harbour facilities in Japan" (MLIT, 2020), the "engineering bedrock" includes the volume of soil in which the effects of non-linearity of soil response are expected to be non-negligible; in our case study it has been assumed to be at the depth of 58 m where the transition between Unit AES7-1 and AES7-2 is located, and where the depth is high enough to include all the soil interacting with the retaining wall. Moreover, the deformation induced by the seismic motions justify the use of a 1D linear-equivalent analysis extended down to the seismic bedrock. In summary, the adoption of an equivalent-linear 1D model to account for the site response in the deeper soil layers enables a reduction in the extent of the FE model, focusing computational efforts on the zones where non-linear soil behavior and soil-structure interaction are most significant. Therefore, in line with the procedure suggested by Mejia and Dawson (2006), the seismic motions representative of the site seismicity have been applied to seismic bedrock in the 1D equivalent-linear model to obtain the upward propagating seismic signals at the engineering bedrock. These seismic signals have been applied at the base of a 1D non-linear model to obtain the equivalent acceleration according to Eurocode 8 and to a 2D model for non-linear dynamic analysis of the geotechnical system. Also, the same 2D model, has been adopted to carry out a pseudo-static analysis aimed at evaluating the capacity curve of the geotechnical system, the value of the critical acceleration and the evaluation of internal stresses related to the application of the equivalent acceleration indicated by the Eurocode 8.

3.5.1. 1D equivalent-linear analysis

The 1D Equivalent-linear Analysis, performed with the STRATA software (Kottke & Rathje, 2009), considered the entire stratigraphy (i.e. extended up to the seismic bedrock which is located at a depth of 350 m) for the evaluation of the upward-propagating seismic signal at the

Table 1
Properties of the 7 chosen seismic motions.

n.	Magnitude (M_w)	Epic. Dist. (km)	Scaling factor (–)	D_{5-95} (s)	Source file name
1	6.00	24	2.55	9.34	ESD 000764xa.cor
2	6.87	11	0.64	31.94	ESD 000182xa.cor
3	6.20	32	1.57	9.38	ESD 000234ya.cor
4	6.19	39	2.69	8.91	NGA 0455 t.txt
5	6.69	61	2.14	17.68	NGA 1033y.txt
6	6.60	36	1.54	12.93	KNET1SAG0010503202153.NS
7	6.30	102	0.37	35.66	20090406_013239ITDPC_ASS_NSC.dat

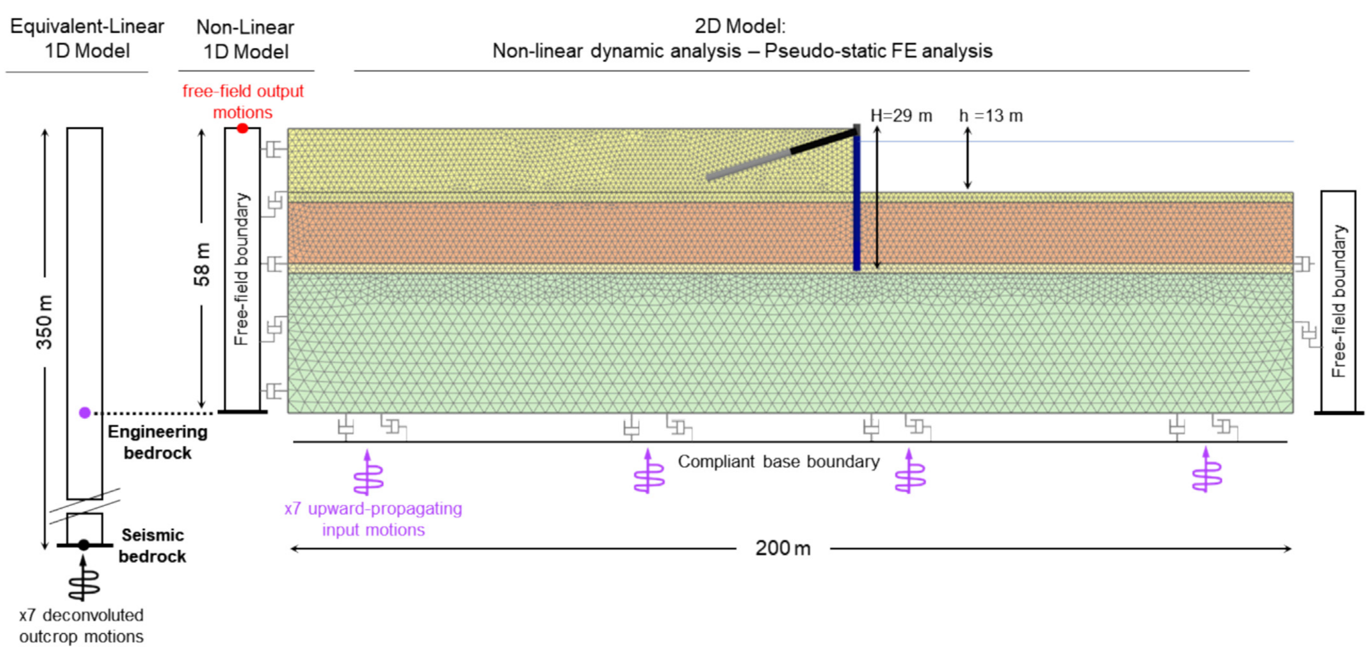

Fig. 4. Models adopted for the numerical analyses: Equivalent-linear 1D model of the whole stratigraphy; Non-linear 1D and 2D models limited to the volume of interest of the quay wall.

assumed engineering bedrock. These seismic signals are then adopted as input for 1D and 2D non-linear time domain analyses. As known, the equivalent-linear analysis is a robust and well-established method for performing site response analyses.

The input parameters are listed in Table 2.

3.5.2. 1D non-linear analysis

The 1D non-linear analysis has been performed on PLAXIS (Bentley, 2023) both to evaluate the free-field ground motion and the average value of equivalent acceleration to be used for pseudo-static analysis according to Eurocode 8.

Table 2
Input parameter for STRATA model.

Layer	Thick. (m)	Unit Weight (kN/m^3)	Plastic Index (–)	p'_{ref} (kPa)	V_S (m/s)	G/G_0 and damping model
S	14.5	18	0	–	77–178	Seed & Idriss (1970)
M	13	19	15	–	145–193	Vucetic & Dobry (1991)
T	2	19	0	–	215	Seed & Idriss (1970)
AES7-1	28.5	20	15	411	240	Darendeli (2001)
AES7-2	53.5	21	15	855	240	
AES6	70	21	5	1546	270	
AES	170	21	5	2889	350	

The constitutive model adopted for all soils was the Hardening Soil with Small-Strain Stiffness model (HSsmall), which can develop hysteretic damping during cyclic loading. The HSsmall model parameters are the same adopted for the 2D non-linear dynamic analysis described in the following section.

The free-field ground motion parameters at surface are summarized in Table 3 in terms of peak ground acceleration (PGA), mean period of the ground motion (T_m), Arias intensity (I_A) and significant duration ($D_{5\text{-}95}$).

3.5.3. 2D FEM non-linear dynamic analysis

The Non-linear Dynamic Analyses of the geotechnical system under investigation were carried out by means of a 2D plain-strain finite element model, using the software PLAXIS. In the model, soil layers within the volume of interest, sheet pile wall, top beam and grouted anchors were included.

The constitutive model adopted for all soils was the Hardening Soil with Small-Strain Stiffness model (HSsmall). For the dynamic phases, a small amount of viscous damping (i. e. 1 %) was added through a Rayleigh formulation in order to account for the dissipation that happens at very small shear-strain levels. The HSsmall model parameters listed in Table 4 were defined through a calibration procedure. The reference initial shear modulus G_0^{ref} and the parameter m (which regulates the stiffness moduli stress dependency) were selected to fit the shear wave velocity profile with depth from Seismic cone and Resonant Column tests (RC), as shown in Fig. 5a. The parameter $\gamma_{0.7}$ (which regulates the strain-dependency of shear stiffness reduction and damping behavior) was chosen to give the best possible approximation of both the normalized shear modulus (G/G_0) decay and damping ratio (D) curves based on RC test results for Silty Sand and Clayey Silt units (Fig. 5b). It is important to note that the damping ratio (D) in the HSsmall model is directly defined from the assigned shear modulus decay curve and cannot be further adjusted. As a result, the calibration of the damping curve does not seem optimal for the Clayey Silt layer, which produces values higher than those of the reference curves for strains $\gamma > 0.01\%$. However, as stated in Callisto et al. (2013), it should be considered that in a time-domain non-linear numerical analysis, the D values are only engaged at the instants of peak strains, making it unlikely to induce excessive overdamping. The calibration procedure followed to define the other model parameters listed in Table 4, which also regulate the soil-structure interaction under static conditions, is not presented here for brevity as it is described in Alesiani and Ruggeri (2024).

Regarding the structural elements, the sheet pile wall and the top beam were modelled as linear-elastic 5-node Mindlin beam elements. The grouted anchor free length was modelled as node-to-node element (elastic spring) and the anchor foundation as embedded beam element (i.e. Mindlin beam elements allowing for relative beam-soil displacements useful for repetitive structural elements in the out-of-plane direction, see Bentley, 2023). The soil-sheet pile wall interface was modelled by using interface elements with a shear strength reduced to 2/3 of the soil strength (i. e. $R_{int} = 0.67$).

The 2D FE mesh (Fig. 3) consisted of triangular 15-node elements and was adopted both for non-linear dynamic and pseudo-static analysis. The maximum element size of the FE mesh was chosen to allow for the correct propagation of the input waves, avoiding unwanted filtering effects on the frequency range of interest. Considering an average distance between two adjacent nodes in a finite element of 0.5 m and a minimum shear wave velocity of approximately 100 m/s in the shallow soil layer, the model can accurately propagate to surface frequencies up to about 20 Hz, following the recommendations of Kuhlemeyer and Lysmer (1973). The lateral vertical boundaries were placed sufficiently far from the retaining structure and the so-called free-field boundaries were adopted to reduce spurious wave reflections and properly simulate the site response. At the model bottom was assigned a compliant base boundary condition, that allows for the upward-propagating input motions to be applied while the incoming waves are absorbed. The model base was set at a depth of 58 m from the surface, where the engineering bedrock was placed for the non-linear site response

Table 3
Free-field surface motion parameters.

n.	PGA (g)	T_m (s)	I_A (m/s)	$D_{5\text{-}95}$ (s)
1	0.120	0.35	0.25	10.9
2	0.129	0.78	0.56	34.6
3	0.098	0.67	0.23	11.7
4	0.113	0.44	0.34	12.0
5	0.082	0.93	0.39	18.8
6	0.089	0.95	0.33	15.0
7	0.084	0.97	0.80	42.8

Table 4
Geotechnical characterization of the low depth units: HSsmall model parameters.

Parameter	Unit	Silty Sand	Clayey Silt	T-Sand	All. Soil
γ	kN/m^3	18	19	19	20
G_0^{ref}	kN/m^2	55,000	60,000	55,000	115,000
$\gamma_{0.7}$	%	0.02	0.02	0.02	0.025
ν_{ur}	–	0.2	0.25	0.2	0.2
E_{50}^{ref}	kN/m^2	12,000	6200	12,000	16,000
E_{oed}^{ref}	kN/m^2	12,000	3100	12,000	16,000
E_{ur}^{ref}	kN/m^2	36,000	24,000	36,000	48,000
p^{ref}	kN/m^2	50	100	50	100
m	–	0.5	1.0	0.5	0
c'	kN/m^2	0	0	0	0
φ'	°	36	31	36	31
ψ	°	0	0	0	0
K_0^{nc}	–	0.412	0.485	0.412	0.485

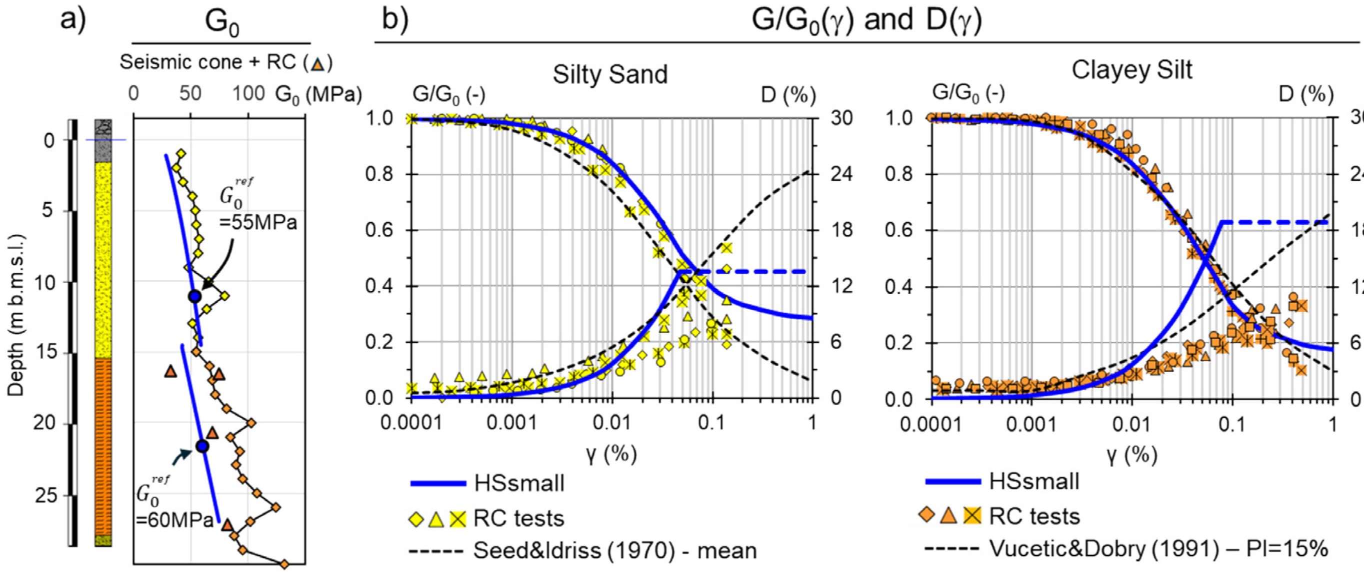

Fig. 5. Calibration of the hysteretic soil model (HSsmall): a) initial shear modulus (G_0) profile fitted on seismic cone and Resonant Column (RC) tests; b) normalized secant shear modulus (G/G_0) decay curve and damping ratio (D) variation curve with shear strain for Silty Sand and Clayey Silt.

effects. However, being the seismic bedrock located at 350 m, the input seismic motion for dynamic phases was taken from the 1D equivalent-linear analysis previously described.

The numerical analysis consisted of two main stages: i) a static stage including structure installation and soil excavation to the operative seabed depth, performed as drained analyses; ii) a time-domain dynamic stage with the application of the 7 input motions, performed after the static stage.

The groundwater level has been assumed to coincide with the mean sea level, pseudo-static and dynamic analyses have been carried out assuming drained conditions for all soils except for the Clayey Silt layer, where undrained conditions have been considered. The hydro-dynamic action of free water in front of the quay wall was not included in the model, as studies have shown it typically has a minor influence on the response of embedded walls (Gazetas et al., 2016).

3.5.4. 2D FE pseudo-static analysis

The pseudo-static analysis was carried out applying to the described 2D finite-element model uniform body forces proportional to the horizontal ground acceleration a_H. Following this method three suite of analyses were carried out: i) the application of the equivalent acceleration values evaluated according to the Eurocode; ii) the construction of the capacity curve by progressively increasing the horizontal ground acceleration; iii) the identification of the critical acceleration of the soil-wall system.

4. Results and discussion

In this section, the main results of the numerical analyses are presented and discussed. The results of internal stresses and permanent displacements obtained by the non-linear 2D FEM Dynamic Analysis are taken as a reference to evaluate the results of the simplified seismic analysis.

4.1. 2D FEM non-linear dynamic analysis

The 2D Non-linear Dynamic Analyses provide the entire history of soil-structure interaction under seismic loading, in term of stress and deformation of both soil and structure. Under the engineering perspective, the maximum internal stresses induced on the structure and the permanent displacements of the wall are the aspects of major interest.

In Fig. 6 the time-histories of maximum bending moment on the sheet pile wall and top beam horizontal displacement induced by the 7 applied accelerograms are shown. It is possible to note a concentration of the bending moment increment in a short time interval, followed by a more gradual further increase until the end of the significant duration of the motion.

As expected for retaining walls an accumulation of displacement is observed, due to the non-symmetric geometry of the problem which favors the movements towards the dredge side while the backward movement is prevented. It is worth noting that the accelerograms 1 and 2 have a similar PGA but determine a very different response on the geotechnical system. Also, the accelerogram 5 has a smaller peak acceleration than n.1 but determines a similar effect in terms of maximum bending moment and permanent displacements. Such observations demonstrate the relevance of mean period of the ground motion (T_m) and Arias intensity (I_A) in determining the response of the geotechnical system. The significant wavelength of the earthquake (which is proportional to T_m) compared to the wall height, determines the synchronous or asyn-

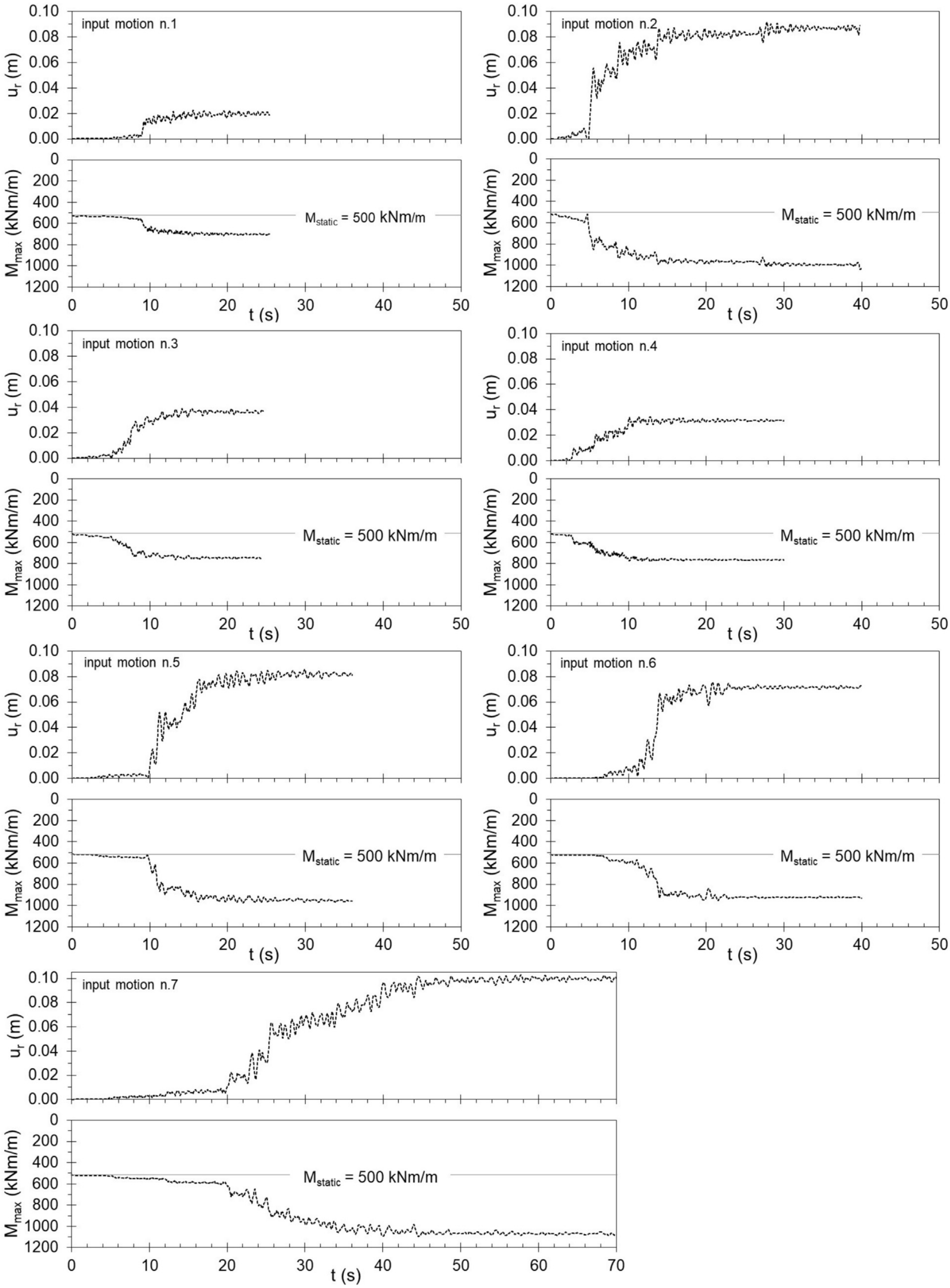

Fig. 6. Time-histories of maximum bending moment on the sheet pile wall and horizontal displacement with time of the top beam induced by the 7 applied seismic motions.

chronous distribution of ground accelerations along the wall, while the Arias Intensity can be related to the number of effective cycles that contribute to the accumulation of wall displacements toward the dredge side.

The maximum displacement is close to 100 mm, that is 0.3 % of the total height of the wall and 0.8 % of the excavation depth. Such value appears tolerable for a flexible retaining wall of an operative quay wall. Note that the "Seismic design guidelines for port structures" (MarCom, 2001) indicate that a residual post seismic displacement up to 1.5 % of the excavation depth still allows regular operation of the quay (i.e. level of damage: Degree I).

In Fig. 7 the bending moment distributions on the retaining wall in the time instant of peak stress, for the 7 accelerograms, are shown. In the same graph the bending moment distribution in the static condition is indicated, for comparison. It is possible to note a maximum value ranging from 700 to 1100 kNm/m for the 7 seismic signals, with a mean value of 850 kNm/m. The difference among the 7 seismic signals is important but expected in relation to their selection based on the spectral matching method, where only the average value of the dynamic analysis suite is significant for the design.

If we consider a static bending moment of around 500 kNm/m, the seismic increment appears relevant but expected for the design situation and the medium–low seismicity of the area. It is worth noting that operative quays are designed for large operative loads that produce a similar increase of internal stresses.

4.2. 2D FE pseudo-static analysis

4.2.1. Eurocode 8

By applying the formula (2) to the 1D Non-linear analysis is possible to evaluate the equivalent acceleration

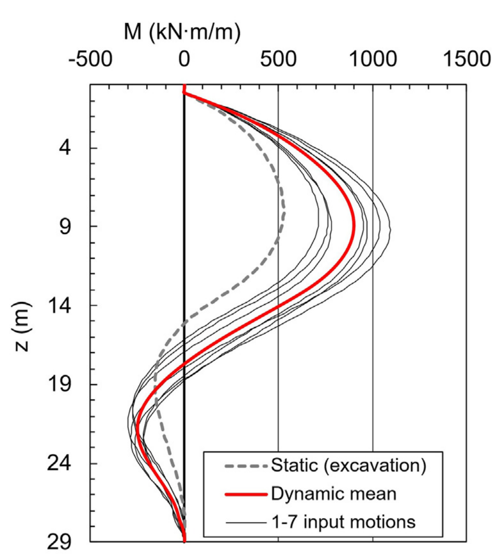

Fig. 7. Bending moment distribution on the quay wall obtained after dynamic analyses with the 7 accelerograms; the bending moment in static condition is also represented for comparison.

according to Eurocode 8. In the particular case of anchored retaining walls with large embedment depth, it may be appropriate to limit the value of reference depth H to a depth smaller than the entire length of the retaining wall, to avoid possible excessive averaging of the seismic input. For this reason, in addition to the reference depth (H) suggested by the Eurocode (i.e. the entire length of the wall), we decided to assume two more values:

- the height of the excavation (h_{excav})
- the height of the active wedge in static condition (h_{wedge});
- the entire length of the retaining wall (H).

Results of the evaluation are shown in Table 5. As expected, the larger the reference depth is assumed, the smaller the corresponding acceleration value is. This is because of the averaging effect on the spatial variation of horizontal acceleration with depth.

By applying the three values of the equivalent acceleration to the FE mesh, the bending moment distributions on the sheet pile wall are shown in Fig. 8. We obtain maximum values of the bending moment ranging from 700 to 950 kNm/m, that means an increase of 40 % and 90 % compared to the static value.

4.2.2. Capacity curve

The non-dimensional capacity curve of the system is shown in Fig. 9. In the same figure the best fitting hyperbolic curve of Eq. (4), obtained by adopting the coefficients $s_F = 0.07$ and $\alpha = 0.86$, is represented. The critical condition is reached for a displacement at the top of the wall of about 7 % of the excavation height, which confirms the high deformability of the retaining system, justified for sheet-pile walls with deep dredge level and the low soil stiffness. For port structures such level of displacement is not compatible with operational requirements. In these situations, the seismic performance should be evaluated with a method able to account for the displacements accumulated before the full capacity of the retaining system. It is interesting to note that executing an unloading–reloading cycle induces the system stiffening. This means that variable loads (i.e. surcharges on the yard, tidal range) experienced prior to seismic loading contribute to mobilize the resistance resources of the system resulting in a reduced accumulation of pre-failure seismic displacements. However, energy dissipation may be also reduced in this situation.

Table 5
Average value of equivalent acceleration according to new EC8-5 formula (Eq. (2).

Reference depth	H (m)	a_{eq} (g)
h_{excav}	13	0.073
h_{wedge}	18	0.058
H	29	0.048

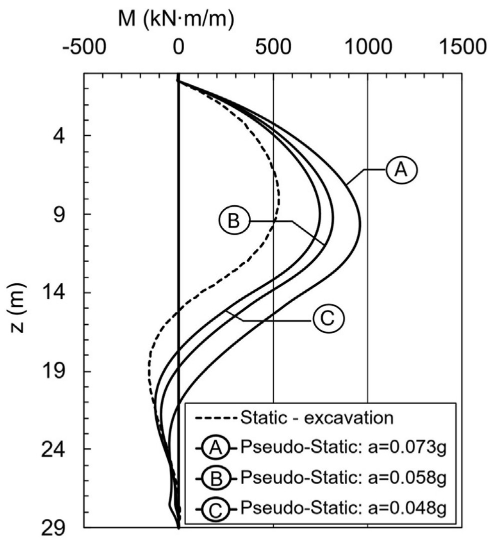

Fig. 8. Bending moment distribution on the quay wall obtained by applying pseudo-static equivalent acceleration according to EC8 for different assumed reference depths.

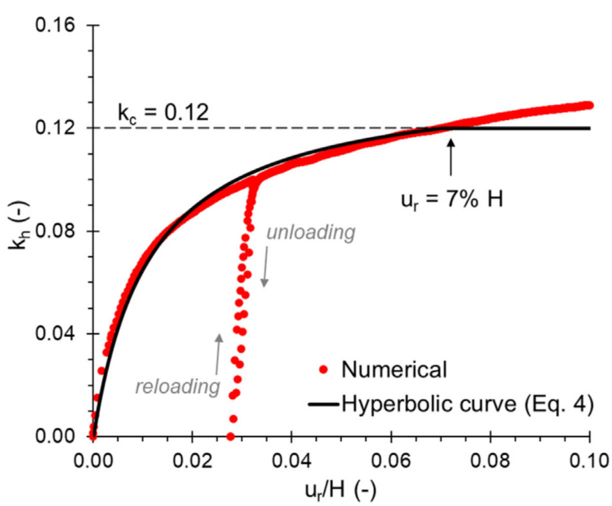

Fig. 9. 2D pseudo-static FE analysis: non-dimensional capacity curve of the soil-wall system.

4.2.3. Critical acceleration and failure mechanism

By progressively increasing the pseudo-static acceleration, the critical acceleration of the geotechnical system was determined. In this context, the critical acceleration is defined as the minimum acceleration capable of activating a failure mechanism of the geotechnical system (i.e. the first plastic mechanism). This first plastic mechanism, illustrated in Fig. 10, was identified at a critical acceleration coefficient of $k_C = 0.12$ which corresponds to a permanent displacement of the wall (u_r) equal to 7 % of its total height (H). The plastic mechanism corresponds to a global failure involving the entire active side of the quay wall system (i.e. the grouted anchor and retaining wall). The shear strains contours (Fig. 10a) within the upper Silty Sand layer clearly outline an active wedge extending to the tip of the grouted anchor, while a zone of diffuse plastic deformation develops in the Clayey Silt layer at the dredge level, due to the restrain provided by the large embedment depth of the sheet-pile wall. As discussed by Callisto and Del Brocco (2015) and Caputo et al. (2021) this mechanism typically occurs in the presence of a robust anchoring system – either in terms of capacity and geometrical layout – which allows the progressive mobilization of the passive resistance of the soil in front of the wall. The relatively small strength increments mobilized during wall rotation account for the slight rise observed in the capacity curve beyond the identified critical acceleration.

The horizontal displacement field at failure shown in Fig. 10b allows to estimate the total mass of soil in motion in the two-dimensional domain ($M = 1414t/m$). the resultant normalized momentum of the soil ($Q_x = 1151t/m$), and the normalized displacement at the top of the wall ($\lambda_x(\boldsymbol{x}_{TOP}) = 0.98$). Then, by applying Eq. (8), it is possible to compute the η^{GN} coefficient required for the GNMH analysis, obtaining a value of $\eta^{GN} \cong 1.2$.

4.3. Internal stresses: Dynamic vs pseudo-static analysis

The bending moment on the sheet pile wall obtained in static condition, the mean value of the 2D Non-linear Dynamic Analyses and the values from the 2D Pseudo-static Analysis carried out according to Eurocode 8 are represented in Fig. 11. Assuming as most accurate the result of the non-linear dynamic analysis, the comparison highlights the good estimation of the maximum bending moment offered by the equivalent static method developed according to EC8; the maximum value of bending moment ranges from 700 to 950 kNm/m that is very similar to the value from non-linear dynamic analysis (i.e. 850 kNm/m).

An aspect that emerges by comparing the distribution of the bending moment is the constraint offered by the embedment length of the retaining wall: static condition and non-linear dynamic results suggest a very effective fixed constraint in the embedment segment, highlighted by the high value of the negative bending moment. Differently, pseudo-static results show a less effective constraint in the embedment, as demonstrated by the reduced value of the negative bending moment that becomes less of the static value. This behaviour may be related to the inherent hypothesis of the equivalent static method in which all the domain of analysis is affected by a constant value of horizontal acceleration.

4.4. Seismic displacements: GNMH vs dynamic analysis

In Fig. 12 the results of the Generalized Newmark Method with Hardening (GNMH) are compared with the permanent displacements obtained by 2D FEM non-linear dynamic analysis for all the 7 seismic motions of interest. For each seismic motion, both the free-field surface motion (black line) and the equivalent accelerogram at the excavation depth (i.e. 13 m from ground level – red line), evaluated by the 1D non-linear Analysis, are

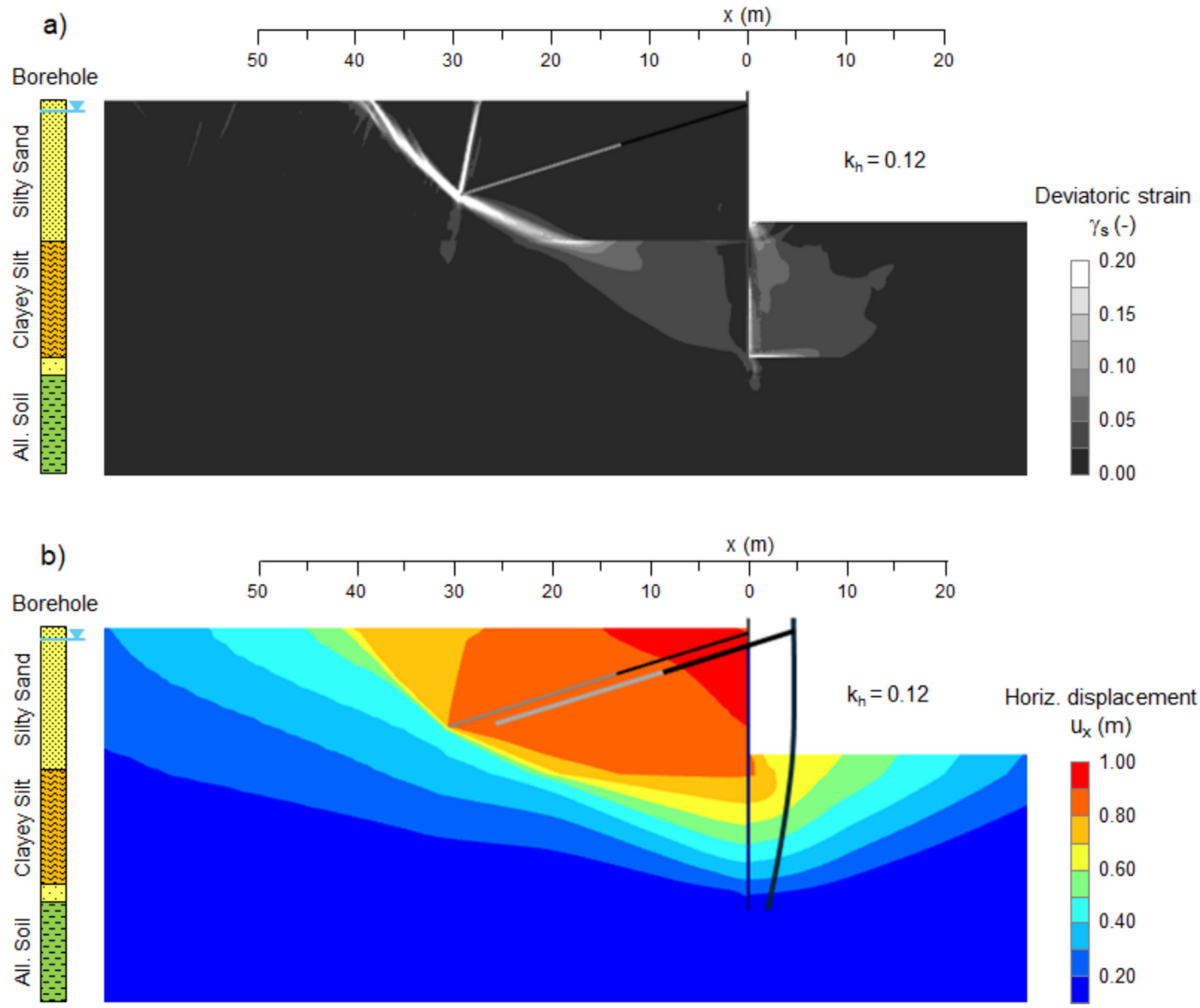

Fig. 10. 2D pseudo-static FE analysis: contours of shear strains (a) and horizontal displacements field (b) at the critical acceleration ($k_h = 0.12$).

shown. Comparison of the time histories reveals that the difference between the two signals varies depending on the seismic motion, being more pronounced in some cases and less in others. For example, considering motions no. 1, 3, and 4, the free-field accelerograms yields displacements up to twice as large as the equivalent ones, while the other motions exhibit differences within 20 %. This variation is attributed to the combined effect of spatial variation and frequency content of the input motions, which have a significant influence on the seismic behavior of the geotechnical system. For each seismic motion, the accumulated wall displacement over time was computed using both the free-field and equivalent accelerograms and then compared with the top wall displacement obtained from 2D non-linear Dynamic Analysis. It is worth noting that the displacement from GNMH align well with those from 2D Dynamic Analysis for all the seismic signals even though the critical acceleration of the system (i.e. $k_h = 0.12$) is rarely exceeded, indicating no permanent displacement would be expected using the traditional Newmark method.

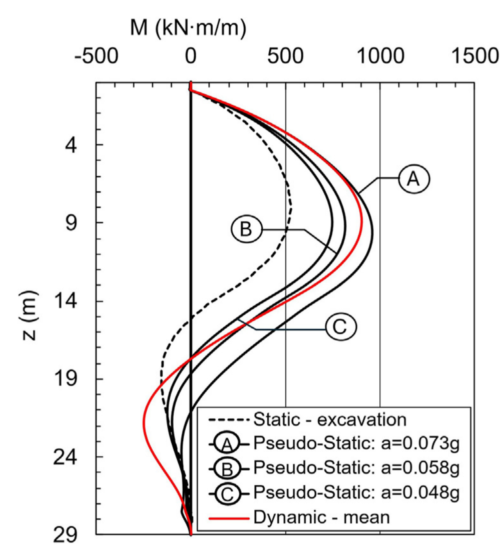

Fig. 11. Comparison between bending moment distribution in Static condition, mean value of Dynamic Analyses and Pseudo-Static Analysis according to EC8 for different assumed reference depths.

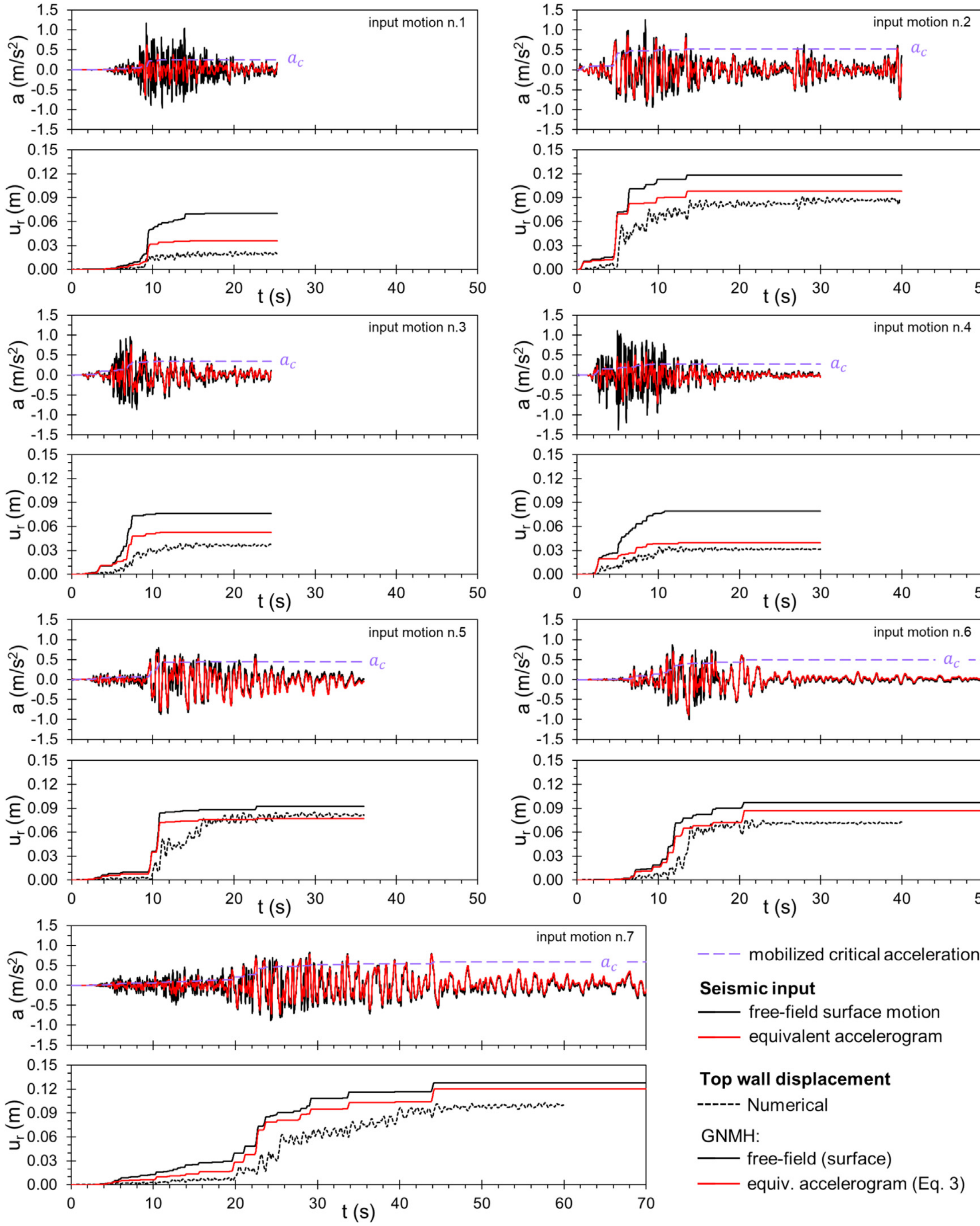

Fig. 12. GNMH method – Time histories of free-field, equivalent accelerograms at the excavation depth and permanent displacement at the top of the wall vs results from non-linear dynamic analysis for the 7 accelerograms.

The best agreement with the 2D Dynamic Analysis is consistently achieved when the equivalent acceleration is considered. This supports the Eurocode 8 assumption that the seismic acceleration acting on the retaining wall corresponds to the average horizontal acceleration over the entire soil column behind it. Conversely, using only the surface free-field motion leads to less accurate predictions, due to the neglect of spatial variation and frequency content of the accelerogram, as demonstrated by the difference between the black and red line.

5. Conclusion

Detailed dynamic numerical analyses appear to be able to capture the seismic behaviour of sheet pile retaining walls of relevant height located in soil of poor properties.

However, this kind of analyses are time-consuming, require an accurate geotechnical characterisation of the site, a comprehensive site response analysis and a lot of care in the choice of seismic ground motions and evaluation of the results. These activities are not yet part of current design practice and seismic analyses based on pseudo-static method are still widely used.

In this work, a seismic evaluation of an existing anchored sheet pile quay wall, performed through a non-linear dynamic numerical analysis, has been compared with the results of simplified seismic methods. Specifically, the pseudo-static method following the procedures suggested by the latest generation of Eurocode 8 for internal stresses, and the recently developed Generalized Newmark Method with Hardening (GNMH) for displacement assessment, were considered. Although the numerical analyses are limited to a single case study and it is assumed that cyclic degradation of soil strength and the liquefaction risk are not relevant, the pseudo-static method proposed by Eurocode 8 proves capable of capturing the key aspects of seismic behavior while maintaining a relatively simple level of model complexity. Furthermore, a good agreement is observed when comparing seismic displacements predicted by the Generalized Newmark Method with Hardening (GNMH) and the non-linear dynamic seismic model, suggesting that GNMH represents a promising tool for evaluating permanent displacements before the full activation of failure mechanisms.

Data availability statement

The data that support the finding of this study are available from the corresponding author upon reasonable request.

CRediT authorship contribution statement

Pierluigi Alesiani: Writing – original draft, Software, Methodology, Investigation, Data curation, Conceptualization. **Paolo Ruggeri:** Writing – original draft, Validation, Supervision. **Viviene M.E. Fruzzetti:** Writing – review & editing, Supervision. **Giuseppe Scarpelli:** Writing – review & editing, Funding acquisition.

References

Alesiani, P., Ruggeri, P., 2024. Assessment of the load test results on a sheet pile quay wall: the potential of the 3D numerical modelling. J. Geotech. Geoenviron. Eng. 150 (9). https://doi.org/10.1061/JGGEFK.GTENG-12368 05024007.

Alesiani, P., Ruggeri, P., Fruzzetti, V.M.E., Scarpelli, G., 2024a. Seismic evaluation of an existing anchored steel sheet-pile quay wall in the Ravenna port (Italy). Japanese Geotechnical Society Special Publication 10 (29), 1110–1115. https://doi.org/10.3208/jgssp.v10.OS-18-07.

Alesiani, P., Ruggeri, P., Scarpelli, G. 2024b. Site-specific seismic coefficient for a quay wall according to the new generation of eurocode 8. In: 18th World Conference on Earthquake Engineering (WCEE2024), Milan, Italy.

Bentley, 2023. PLAXIS Reference Manual: 3D—Connect Edition V23.2.

Callisto, L., 2024. A method for the seismic design of multi-propped retaining walls. Rivista Italiana Di Geotecnica. https://doi.org/10.19199/2024.1.0557-1405.044.

Callisto, L. 2019. On the seismic design of displacing earth retaining systems. In: 7th International Conference on Earthquake Geotechnical Engineering (7ICEGE), Roma, Italy.

Callisto, L., Del Brocco, I., 2015. Intrinsic seismic protection of cantilevered and anchored retaining structures. Proc., SECED Conf. on Earthquake Risk and Engineering towards a Resilient World. Society for Earthquake and Civil Engineering Dynamics, Cambridge, UK.

Callisto, L., Rampello, S., Viggiani, G.M., 2013. Soil–structure interaction for the seismic design of the Messina strait bridge. Soil Dyn. Earthq. Eng. 52, 103–115.

CEN/TC 250/SC 8, 2024. FprEN 1998-5:2024. Eurocode 8: Earthquake resistance design of structures – Part 5: Geotechnical aspects, foundations, retaining and underground structures.

Callisto, L., 2014. Capacity design of embedded retaining structures. Géotechnique 64 (3), 204–214. https://doi.org/10.1680/geot.13.P.091.

Caputo, G., Conti, R., Viggiani, G.M., 2023. Effects of displacement hardening on the seismic design of anchored walls. J. Geotech. Geoenviron. Eng. 149 (11). https://doi.org/10.1061/JGGEFK.GTENG-11442 04023112.

Caputo, G., Conti, R., Viggiani, G.M., Prüm, C., 2021. Improved method for the seismic design of anchored steel sheet pile walls. J. Geotech. Geoenviron. Eng. 147 (2). https://doi.org/10.1061/(ASCE)GT.1943-5606.0002429 04020154.

Cattoni, E., Salciarini, D., Tamagnini, C., 2019. A Generalized Newmark Method for the assessment of permanent displacements of flexible retaining structures under seismic loading conditions. Soil Dyn. Earthq. Eng. 117, 221–233. https://doi.org/10.1016/j.soildyn.2018.11.023.

Cecconi, M., Pane, V., Vecchietti, A., 2015. Seismic displacement-based design of embedded retaining structures. Bulletin Georgian Academy Sci. Earthq. Eng. 13, 1979–2001. https://doi.org/10.1007/s10518-014-9708-8.

Conti, R., Viggiani, G.M., 2023. On the performance-based seismic design of yielding retaining structures. Soil Dyn. Earthq. Eng. 174. https://doi.org/10.1016/j.soildyn.2023.108172 108172.

Darendeli, M.B., 2001. Development of a new family of normalized modulus reduction and material damping curves. The university of Texas, Austin (PhD thesis).

Gazetas, G., Garini, E., Zafeirakos, A., 2016. Seismic analysis of tall anchored sheet-pile walls. Soil Dyn. Earthq. Eng. 91, 209–221.

Iai, S., 2019. Evaluation of performance of port structures during earthquakes. Soil Dyn. Earthq. Eng. 126. https://doi.org/10.1016/j.soildyn.2018.04.055 105192.

Iai, S., Kameoka, T., 1993. Finite element analysis of earthquake induced damage to anchored sheet pile quay walls. Soils Found. 33 (1), 71–91. https://doi.org/10.3208/sandf1972.33.71.

ISPRA, 2009. Geological map of Italy at 1:50,000 scale, Sheet 222 – Lugo [Map, in Italian]. Rome: Italian National Institute for Environmental Protection and Research – Geological Survey of Italy. https://www.isprambiente.gov.it/Media/carg/222_LUGO_SOTTO/Foglio.html.

Kamon, M., Wako, T., Isemura, K., Sawa, K., Mimura, M., Tateyama, K., Kobayashi, S., 1996. Geotechnical disasters on the waterfront. Soils Found. 36 (Special), 137–147. https://doi.org/10.3208/sandf.36.Special_137.

Kayen, R., 2024. Geology is the key: Understanding the liquefaction susceptibility of Niigata City soil. Japanese Geotechnical Society Special Publication 10 (10), 247–252.

Kottke, A.R., Rathje, E.M., 2009. Technical manual for Strata. PEER, Berkeley, California.

Kuhlemeyer, R.L., Lysmer, J., 1973. Finite element method accuracy for wave propagation problems. Journal of the Soil Mechanics and Foundations Division 99 (5), 421–427.

MarCom, PIANC 2001. Seismic design guidelines for port structures. In Working Group (No. 34).

Mejia, L.H., Dawson, W.M., 2006. Earthquake Deconvolution for FLAC. Itasca International, Itasca, NY.

MLIT, 2020. Technical standard and commentaries for port and harbor facilities in Japan. Ministry of Land, Infrastructure, Transport and Tourism (MLIT): Ports and Harbors Bureau.

Mononobe, N., Matsuo, H., 1929. On the determination of earth pressure during earthquakes. Proc. World Eng. Conf., Tokyo 9, 177–185.

Nakajima, S., Koseki, J., Watanabe, K., Tateyama, M., 2009. A simplified procedure to evaluate earthquake-induced residual displacements of conventional type retaining walls. Soils Found. 49 (2), 287–303. https://doi.org/10.3208/sandf.49.287.

Newmark, N.M., 1965. Effects of Earthquakes on Dams and Embankments. Géotechnique 15 (2), 139–160.

Nozu, A., Ichii, K., Sugano, T., 2004. Seismic design of port structures. J. Japan Associat. Earthquake Eng. 4 (3), 195–208. https://doi.org/10.5610/jaee.4.3_195.

Okabe, S., 1926. General theory of earth pressure. J. Japanese Society Civil Eng. 12 (1).

Oliynyk, K., Pontani, N., Tamagnini, C., 2021. On the effects of pore water pressure buildup and dissipation on the seismic performance of a propped rc diaphragm wall in sand. Acta Geotech. 16, 1547–1573.

Oliynyk, K., Conti, R., Viggiani, G., Tamagnini, C., 2022. A generalised Newmark method with displacement hardening for the prediction of seismically induced permanent deformations of diaphragm walls. Géotechnique 74 (8), 774–786.

Pecker, A., 2019. Development of the second generation of Eurocode 8–Part 5: a move towards performance-based design. Earthquake Geotechnical Engineering for Protection and Development of Environment and Constructions. CRC Press, pp. 273–281.

PIANC. 2001. Seismic design guidelines for port structures, Working Group No. 34 of the Maritime Navigation Commission, International Navigation Association, Balkema, Rotterdam, The Netherlands.

Rota, M., Zuccolo, E., Taverna, L., Corigliano, M., Lai, C.G., Penna, A., 2012. Mesozonation of the Italian territory for the definition of real spectrum-compatible accelerograms. Bulletin of the Georgian Academy of SciencesEarthq. Eng. 10, 1357–1375.

Richards, R., Elms, D.G., 1979. Seismic behavior of gravity retaining walls. J. Geotech. Eng. Div. ASCE 105 (4), 449–464.

Seed, H.B., Idriss, I.M. 1970. Soil moduli and damping factors for dynamic response analyses. Technical Report EERC 70-10, Earthquake Engineering Research Center, University of California, Berkeley, CA.

Seed, H.B., Martin, G.R., 1966. The seismic coefficient in earth dam design. J. Soil Mech. Found. Div. 92 (3), 25–58.

Senigagliesi, M., Alesiani, P., Ruggeri, P., Fruzzetti, V.M.E., Scarpelli, G. 2024. Dynamic properties of the Holocene age deposit in the Italian port of Ravenna. In: 7th International Conference on Geotechnical and Geophysical Site Characterization (ISC2024), Barcelona, Spain. https://doi.org/10.23967/isc.2024.23.

Sugano, T., Nozu, A., Kohama, E., Shimosako, K.I., Kikuchi, Y., 2014. Damage to coastal structures. Soils Found. 54 (4), 883–901. https://doi.org/10.1016/j.sandf.2014.06.018.

Sumer, B. Mutlu, Ansal, Atilla, Cetin, K. Onder, Damgaard, Jesper, Gunbak, A. Riza, Hansen, Niels-Erik Ottesen, Sawicki, Andrzej, Synolakis, Costas E., Yalciner, Ahmet Cevdet, Yuksel, Yalcin, Zen, Kouki. 2007. Earthquake-Induced Liquefaction around Marine Structures. J. Waterway, Port, Coastal, Ocean Eng., 133(1), 55–82. https://doi.org/10.1061/(ASCE)0733-950X(2007)133:1(55).

Towhata, I., 2008. Geotechnical Earthquake Engineering. Editors: Wei Wu and Ronaldo I. Borja. Springer, Berlin.

Towhata, I., Ghalandarzadeh, A., Sundarraj, K.P., Vargas-Monge, W., 1996. Dynamic failures of subsoils observed in waterfront areas. Soils Found. 36 (Special), 149–160. https://doi.org/10.3208/sandf.36.Special_149.

Towhata, I., Islam, M.S., 1987. Prediction of lateral displacement of anchored bulkheads induced by seismic liquefaction. Soils Found. 27 (4), 137–147. https://doi.org/10.3208/sandf1972.27.4_137.

Vucetic, M., Dobry, R., 1991. Effect of soil plasticity on cyclic response. J. Geotech. Eng. 117 (1), 89–107.